

A new hierarchic degenerated shell element for geometrically non-linear analysis of composite laminated square and skew plates

Kwang-Sung Woo[†] and Jin-Hwan Park[‡]

Civil Engineering Department, Yeungnam University, Gyeongsan 712-749, Korea

Chong-Hyun Hong[†]

Civil Engineering Department, Tamna University, Seoguipo 697-340, Korea

(Received March 29, 2003, Accepted December 1, 2003)

Abstract. This paper extends the use of the hierarchic degenerated shell element to geometric non-linear analysis of composite laminated skew plates by the p -version of the finite element method. For the geometric non-linear analysis, the total Lagrangian formulation is adopted with moderately large displacement and small strain being accounted for in the sense of von Karman hypothesis. The present model is based on equivalent-single layer laminate theory with the first order shear deformation including a shear correction factor of 5/6. The integrals of Legendre polynomials are used for shape functions with p -level varying from 1 to 10. A wide variety of linear and non-linear results obtained by the p -version finite element model are presented for the laminated skew plates as well as laminated square plates. A numerical analysis is made to illustrate the influence of the geometric non-linear effect on the transverse deflections and the stresses with respect to width/depth ratio (a/h), skew angle (β), and stacking sequence of layers. The present results are in good agreement with the results in literatures.

Key words: geometric non-linearity; laminated skew plates; hierarchic degenerated shell element; integrals of Legendre polynomials; equivalent-single layer laminate theory.

1. Introduction

The analysis of laminated composites requires effective computational techniques such as the finite element method because large displacements and rotations may constitute a major part of the overall motion (Madenci 1994). Especially, the necessity of analyzing non-linear behavior of laminated composite plates and shells arises not only because of their application in modern aerospace and other structures, but also because of the interest in classical problems of bending and instability. However, if the lateral deflection exceeds one-half the plate thickness (Timoshenko 1959), the classical theory of laminated plates is generally not adequate and the second-order effect of the vertical displacements on the membrane stresses needs to be considered. Such tendencies will

[†] Professor

[‡] Researcher

be significant as the lateral deflection is increased, and can be observed in laminated plates as well (Fares 1999, Liu 1997).

The proposed p -version finite element model is a possible alternative to overcome the spurious mechanism like shear-locking as the polynomial order or p -level is increased (Holzer 1996). In this study, the original degenerate shell concept has been partly modified based on the p -version of the finite element method, since the proposed finite element approach is based on the sub-parametric concept (Szabo 1991).

The aim of this paper is to investigate the geometric non-linear effects on the transverse deflections and stresses with respect to width/depth ratio, skew angle, and stacking sequence of layers. In the non-linear formulation of the model, total Lagrangian formulation is adopted with small strains and moderately large deflections. The rotations are accounted for in the sense of von Karman hypothesis. In this formulation, all of the quantities are referred to a fixed configuration, and changes in the displacement and stress fields are determined with respect to the reference configuration. The strain and stress measures used in this approach are the Green-Lagrange strain tensor and 2nd Piola-Kirchhoff stress tensor. The integrals of Legendre polynomials are used for shape functions with p -level varying from 1 to 10.

2. Hierarchic degenerated shell element

In this section, we attempt to formulate a degenerated assumed strain shell element, which employs Lagrangian basis subparametric mapping for geometry and integrals of Legendre polynomials for solution interpolation. The original degenerated shell elements are derived from the equations of three-dimensional continuum mechanics under the basic assumptions of Mindlin theory (Rank 1998). The resulting elements have 5 degrees of freedom at an arbitrary nodal point k located in the middle surface such as three translations (u_{ik}^{mid}) and two rotations (β_{1k}, β_{2k}). In the subparametric formulation of the p -version of the finite element method, the following mapping function based on the shape functions corresponding to the vertex modes only is used. The mapping function (1) is valid for straight sided elements only. Therefore, the shell problem with curved geometry can be discretized with the special mapping technique such as the transfinite mapping technique (Liu 1995).

$$x_i = \sum_{k=1}^{N_c} \Psi_k(\xi, \eta) x_{ik}^{mid} + \sum_{k=1}^{N_c} \Psi_k(\xi, \eta) \frac{h_k}{2} \xi \bar{v}_{3k}^i \quad (1)$$

where $i (= 1, 2, 3)$ refer to the three global directions, h_k is the shell thickness at node k , $\Psi_k(\xi, \eta)$ is the element shape function based on integrals of Legendre polynomials, N_c is the number of vertex modes, and \bar{v}_{3k}^i is constructed from the nodal coordinates of the top and bottom surfaces at node k that refers to the vector component in the global coordinates system. Also, ξ, η, ζ are curvilinear coordinates, as shown in Fig. 1.

The displacement field can then be expressed in terms of mid-point translations u_{ik}^{mid} and mid-point rotations β_{ik} :

$$u_i = \sum_{k=1}^{N_p} \Psi_k(\xi, \eta) u_{ik}^{mid} + \sum_{k=1}^{N_p} \Psi_k(\xi, \eta) \frac{h_k}{2} [\bar{v}_{1k}, -\bar{v}_{2k}] \begin{bmatrix} \beta_{1k} \\ \beta_{2k} \end{bmatrix} \quad (2)$$

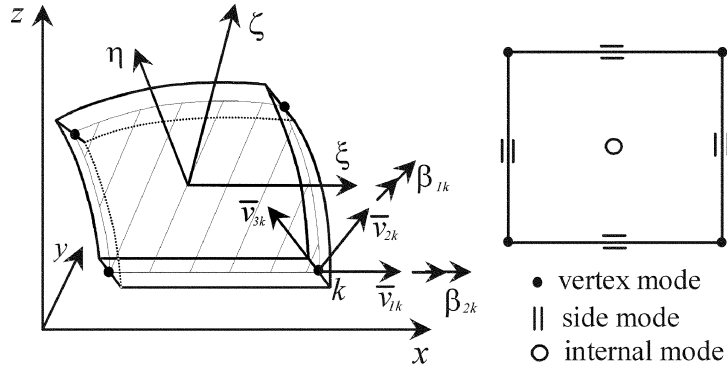


Fig. 1 Coordinate systems in degenerate shell element

where \bar{v}_{1k} , \bar{v}_{2k} are unit vectors in the global coordinates system at node k , and N_p is the number of unknowns with respect to increase of p -level. Since N_p is greater than N_c , except when p -level is equal to 1, the proposed hierachic degenerated shell element is basically constructed by sub-parametric element concept.

The hierachic shape function $\Psi_k(\xi, \eta)$ requires to be orthogonal in energy norm and recurrent (Woo 1993), as represented by, say, integrals of Legendre polynomials. They can be grouped into three classes. The first group is the basic mode or the vertex mode, which are the usual shape functions for bilinear elements when p -level = 1. The second group is side modes (*a.k.a.* edge modes). For a 2-D case, $P_n(\xi)$ and $P_n(\eta)$ are multiplied by the factors $(\eta - 1)$, $(\xi + 1)$, $(\eta + 1)$, $(\xi - 1)$ along edges $\xi = \pm 1$ and $\eta = \pm 1$, respectively, in order to obtain a sequence of hierachic shape functions. Thus the side mode of the quadrilateral element for each higher p -level is required to be added as;

$$\begin{aligned}\Psi_i(\xi, \eta) &= (1 \pm \eta) \cdot P_n(\xi) \quad \text{for } \eta = \pm 1 \\ \Psi_i(\xi, \eta) &= (1 \pm \xi) \cdot P_n(\eta) \quad \text{for } \xi = \pm 1\end{aligned}\quad (3)$$

where

$$P_n(x) = \sqrt{\frac{2n-1}{2}} \int_{i=-1}^x L_{i-1}(t) dt \quad (4)$$

where $L_n(t)$ is the Legendre polynomial defined by Rodrigues' formula. The third class is the bubble mode or the internal mode defined by

$$\Psi_i(\xi, \eta) = P_i(\xi) \cdot P_j(\eta), \quad i, j \geq 2 \quad (5)$$

which are identically zero on all edges of the elements. The completeness requirement is satisfied by introducing the bubble mode or the internal mode for $p \geq 4$ as $P_i(\xi) \cdot P_j(\eta)$ with the requirement that $i + j = p$ and $i, j \geq 2$.

3. Equivalent-single layered model

In the equivalent single-layer theories, on reducing the three-dimensional elasticity problem to a two-dimensional problem, the laminate is characterized as an equivalent, homogeneous layer. Therefore, the number of governing equations is not dependent on the number of layers comprising a laminate. Although, these theories account for continuous transverse strains through the thickness, they predict discontinuous stress distributions at the layer interfaces due to dissimilar properties of adjacent layers. As a result, a post-processing procedure is usually required to recover the actual interlaminar stress state by integrating the equilibrium equations.

The strain components, defined by the Green-Lagrangian strain tensor, are obtained from the displacements applying the conditions of kinematic compatibility, including quadratic terms accounting for finite displacements. However, the von Karman's strain-displacement relationship for moderately large deflection analysis can be considered as a special case of Green's strain tensor. Thus the in-plane strain terms for a plate in the x - y plane, denoted by $(\partial u / \partial x)^2$, $(\partial v / \partial x)^2$, $(\partial u / \partial y)^2$ and $(\partial v / \partial y)^2$, are considered negligible in this work. Such that,

$$\boldsymbol{\varepsilon}_{ij} = \begin{bmatrix} \varepsilon_x \\ \varepsilon_y \\ \gamma_{xy} \\ \gamma_{xz} \\ \gamma_{yz} \end{bmatrix} = \begin{bmatrix} \frac{\partial u}{\partial x} \\ \frac{\partial v}{\partial y} \\ \frac{\partial u}{\partial y} + \frac{\partial v}{\partial x} \\ \frac{\partial u}{\partial z} + \frac{\partial w}{\partial x} \\ \frac{\partial v}{\partial z} + \frac{\partial w}{\partial y} \end{bmatrix} + \begin{bmatrix} \frac{1}{2} \left(\frac{\partial w}{\partial x} \right)^2 \\ \frac{1}{2} \left(\frac{\partial w}{\partial y} \right)^2 \\ \frac{\partial w}{\partial x} \frac{\partial w}{\partial y} \\ 0 \\ 0 \end{bmatrix} \quad (6)$$

It is convenient to distinguish between the linear part $\boldsymbol{\varepsilon}_l$ and non-linear part $\boldsymbol{\varepsilon}_{nl}$ so that $\boldsymbol{\varepsilon} = \boldsymbol{\varepsilon}_l + \boldsymbol{\varepsilon}_{nl}$.

The discretization procedures of the weak form can be done by Galerkin method, according to a standard methodology (Actis 1999). If the deformation process is divided into sequential equilibrium states with configurations corresponding to M domains like $\Omega_{(1)}, \Omega_{(2)}, \dots, \Omega_{(M)}$, and N boundaries like $\Gamma_{(1)}, \Gamma_{(2)}, \dots, \Gamma_{(N)}$, the incremental linearized equation of equilibrium can be expressed in the following form:

$$(K_{ik}^D + K_{ik}^G)^r \cdot \Delta u_k^{(r+1)} = (f_i^{ex})^s - (f_i^{in})^r \quad (7)$$

with

$$K_{ik}^D = \int_{\Omega_{(M)}} \Psi_{i,j} C_{ijkl} \Psi_{k,l} d\Omega \quad (8)$$

$$K_{ik}^G = \int_{\Omega_{(M)}} \Psi_{i,j} \delta_{jl} \sigma_{jl} \Psi_{k,l} d\Omega \quad (9)$$

$$f_i^{ex} = \int_{\Gamma_{(N)}} \Psi_i T_i d\Gamma \quad (10)$$

$$f_i^{in} = \int_{\Omega_{(M)}} \Psi_{i,j} \sigma_{ij} d\Omega \quad (11)$$

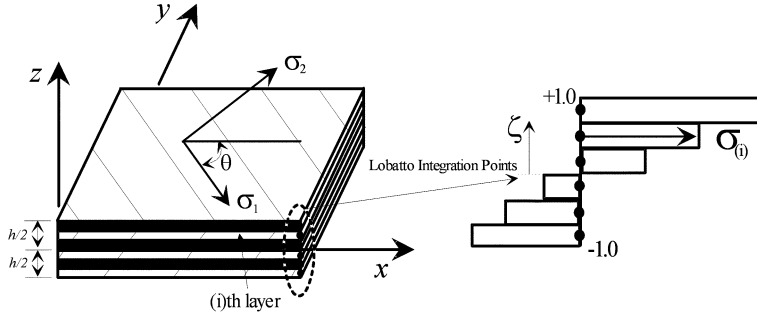


Fig. 2 Layered model with inclination of the principal axes of anisotropy

where K^D, K^G are called the material and geometry stiffness matrices, respectively; $\Delta u_k^{(r+1)}$ denotes the solution vector obtained in the $(r+1)$ -th iteration; f^{ex}, f^{in} are the nodal force vectors due to imposed boundary and internal forces in the r -th iteration. Also, C_{ijkl} and s are the elastic modulus with the fourth rank tensor and the stage of load increment, and T_i is the traction vector along the boundary. The above incremental matrix is solved by the tangential stiffness method.

Layers are numbered sequentially, starting at the bottom surface of the laminated plate. Since the equivalent-single layer (ESL) theory with the first order shear deformation including a shear correction factor of 5/6 is adopted in this study, the stress components of the layer are computed at the stress points on the mid-surface of layer, and are assumed to be constant over the thickness of each layer, so that the actual stress distribution of the laminated plate is modeled by a piecewise constant approximation shown in Fig. 2. If the principal axes of anisotropy 1, 2 do not coincide with the reference axes x, y , but are rotated by a certain angle θ , the relationship between the components of stress in two coordinate direction can be defined by:

$$(\sigma_{kl})_m = a_{ki}a_{lj}(\sigma_{ij})_p \quad (12)$$

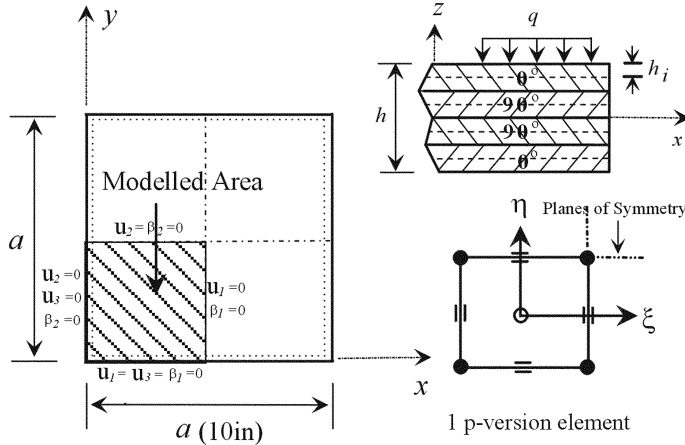
$$(\sigma_{kl})_p = a_{ik}a_{jl}(\sigma_{ij})_m \quad (13)$$

where $(\sigma_{ij})_m$ are the components of the stress tensor in the material coordinates of anisotropy, $(\sigma_{ij})_p$ are the components of the same stress tensor in the problem or reference coordinates system, and a_{ij} are the direction cosines. It is also necessary to transform the element matrices corresponding to rectangular axes along which the oblique edges are specified in the skew plates.

4. Numerical examples

4.1 Laminated anisotropic square plates

The first example is a simply supported square laminated plate subjected to a uniformly distributed load q with four different cross-ply angles. To investigate thickness effect, the width/depth ratio, a/h , is selected as 10 for thick case, and 100 for thin case. Each lamina has the same thickness $h_i = h/8$ as shown in Fig. 3, where h is the thickness of laminated plates and a is the

Fig. 3 Geometry of laminated anisotropic plates and p -version finite element model

length of the plate. One quadrant of the laminate is discretized by a single p -version finite element with suitable boundary conditions as shown in Fig. 3. The following non-dimensional bending response characteristics are used throughout the figures:

$$M_{xx}^* = M_{xx}(a/2, a/2)a/E_2 h^4, \quad M_{yy}^* = M_{yy}(a/2, a/2)a/E_2 h^4, \quad \sigma_{xx}^* = \sigma_{xx}(a/2, a/2)a/E_2 h,$$

$$\sigma_{yy}^* = \sigma_{yy}(a/2, a/2)a/E_2 h, \quad q^* = qa^3/E_2 h^3, \quad w^* = w(a/2, a/2)/h$$

The material properties given in Table 1 correspond to a high modulus graphite/epoxy composite (Owen 1983, Schwartz 1992). These data may serve only to undertake parametric studies and numerical tests.

The present results obtained by the single p -version finite element model are compared with the theoretical results proposed by Reddy (1984, 1997) based on Sanders' shell theory, and the numerical results obtained by Owen (1983, 1987) using Heterosis element. As shown in Table 3, the p -version solutions agree very well with those in literature with respect to the plate thickness and different cross-ply with fiber orientations of Case I ($0^\circ/90^\circ/90^\circ/0^\circ$) and Case II ($0^\circ/0^\circ/90^\circ/90^\circ$) as defined in Table 2. It is noted that the NDF (number of degrees of freedom) requirement of the

Table 1 Material constants for laminated anisotropic plates (unit: ksi)

Material constants	E_1	E_2	G_{12}	G_{13}	G_{23}	ν_{12}
Anisotropic Graphite/Epoxy	25000	1000	500	500	200	0.25

Table 2 Stacking sequence for numerical examples

Example	Case I	Case II	Case III	Case IV
Ply angle	$0^\circ/90^\circ/90^\circ/0^\circ$	$0^\circ/0^\circ/90^\circ/90^\circ$	$0^\circ/0^\circ/0^\circ/0^\circ$	$0^\circ/90^\circ/0^\circ/90^\circ$

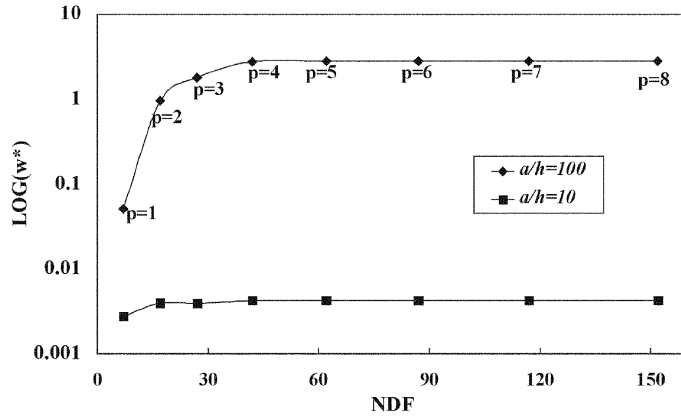


Fig. 4 Convergence characteristics of normalized central deflection of laminated anisotropic square plates for Case I

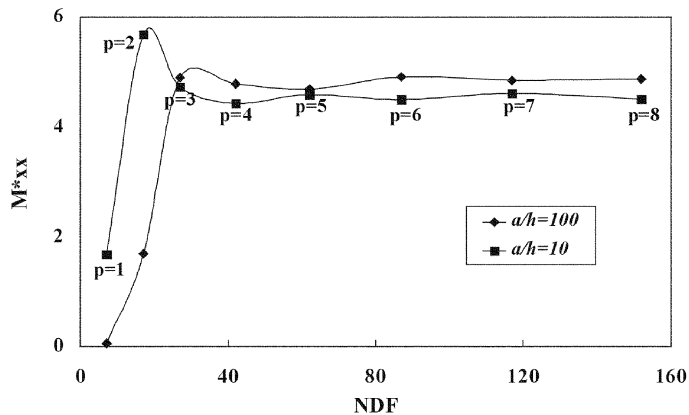


Fig. 5 Convergence characteristics of normalized central moment of laminated anisotropic square plates for Case I

Table 3 Normalized center deflections with respect to a/h ratio and stacking sequence when $q^* = 1.0$

Cross-Ply	a/h	Linear			Geometric Non-linear	
		Reddy (Theoretical)	Owen (NDF=153)	p -version (NDF=62)	Owen (NDF=153)	p -version (NDF=62)
Case I (0°/90°/90°/0°)	100	0.683	0.688	0.693	0.617	0.620
	10	0.102	0.103	0.096	0.103	0.096
Case II (0°/0°/90°/90°)	100	1.698	1.741	1.768	0.754	0.754
	10	0.194	0.201	0.199	0.197	0.193

p -version solution obtained by a single element has been found to be 62 at p -level = 5 as compared to 153 with 9 uniform Heterosis elements by Owen to achieve the same level of accuracy as shown in Table 3. In this study, the influence of the thickness ratio and stacking sequence on the central deflection w^* and central moment M_{xx}^* and M_{yy}^* is shown in Figs. 6-7 and 9-10, respectively.

In comparison with the linear analysis, the normalized center deflections by geometric non-linear analysis are reduced for thin plates, but not noticeable for thick plates. In other words, the influence of the geometric non-linear effect (or second-order effect) on the lateral deflections is more pronounced for thin plates. From Table 3, it is also seen that the deflection for symmetric stacking sequence (Case I) is smaller than that for non-symmetric stacking sequence (Case II).

A wide variety of linear and non-linear results are presented for laminated anisotropic plates with different four cross-ply cases. Figs. 6 and 7 show linear and non-linear load-deflection curves for different fiber orientations. These figures reveal that the effect of geometric non-linearity is more significant for thin plates with non-symmetric stacking sequence. In addition, the non-linear load-deflection curves converge with increasing the number of layers as shown in Fig. 8. Thus the laminated plate has been divided by eight lamina such as $h_i = h/8$ where h is the thickness of laminated plates. This indicates that the coupling effect between bending and extension decreases.

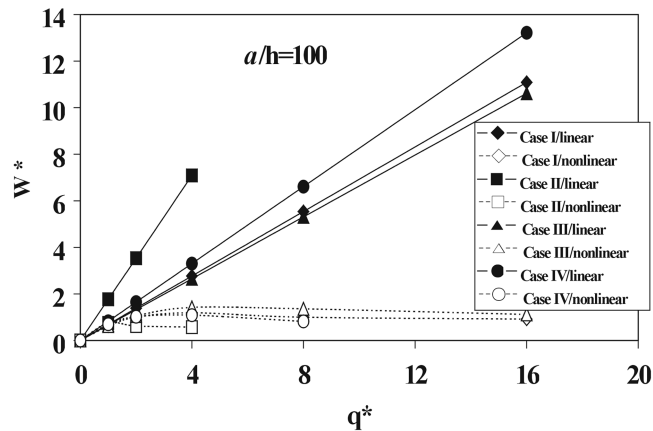


Fig. 6 Normalized load/central deflection characteristics by linear and non-linear analyses for thin plates ($a/h = 100$)

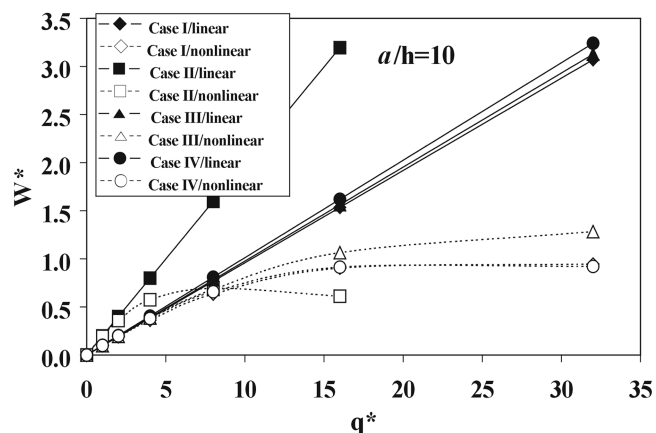


Fig. 7 Normalized load/central deflection characteristics by linear and non-linear analyses for thick plates ($a/h = 10$)

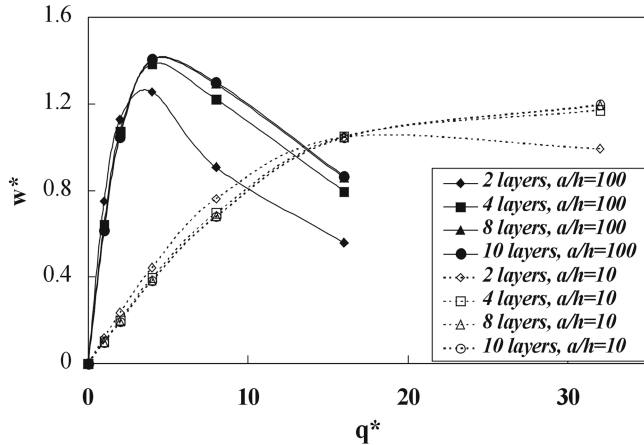


Fig. 8 Convergence characteristics of nonlinear load-deflection with respect to the number of layers for Case III

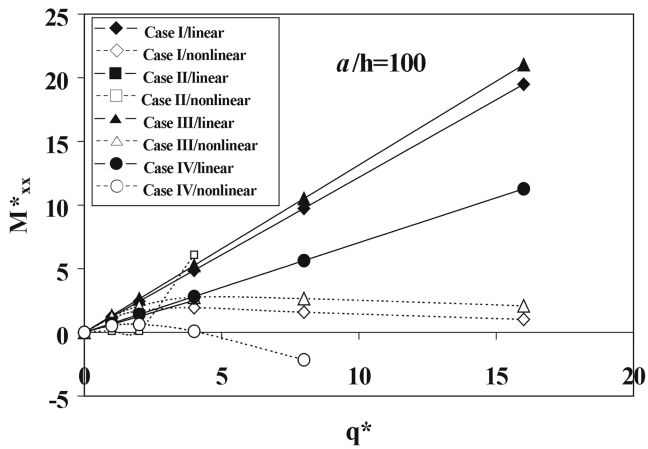


Fig. 9 The non-linear behavior of normalized central moment M_{xx}^* for thin plates ($a/h = 100$)

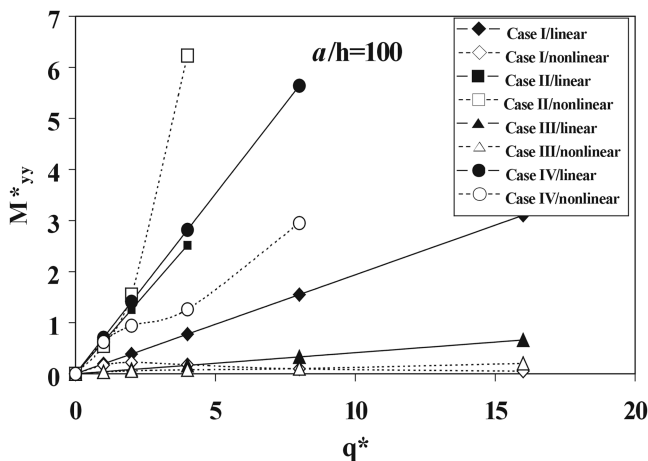


Fig. 10 The non-linear behavior of normalized central moment M_{yy}^* for thin plates ($a/h = 100$)

The normalized moment M_{xx}^* and M_{yy}^* have been plotted in Figs. 9-10 for thin laminated anisotropic plates. For thin plates, the normalized moments along x -axis and y -axis show the importance of geometrically non-linear analysis since the normalized moments become smaller as the geometric non-linearity is considered only except for Case II.

Also, the non-linear response for w^* , M_{xx}^* , M_{yy}^* against a/h ratio and q^* are shown in the tabulated forms between Table 4 and Table 7. Even though there are some unstable numerical values of M_{xx}^* and M_{yy}^* , these tables will be useful and used for comparison with future results on this objective.

From these results, the load-deflection curves and load-stress curves indicate that the inclusion of the effect of geometric non-linearity contributes more significantly in the cases of laminated thin

Table 4 Normalized value of laminated anisotropic square plates for Case I

q^*	a/h	Nonlinear response		
		w^*	M_{xx}^*	M_{yy}^*
1.0	10	0.096(0.096)	0.114(0.115)	0.025(0.025)
	100	0.620(0.690)	1.093(1.228)	0.167(0.197)
2.0	10	0.189(0.192)	0.226(0.229)	0.049(0.049)
	100	0.997(1.388)	1.695(2.436)	0.224(0.388)
4.0	10	0.362(0.384)	0.432(0.459)	0.092(0.099)
	100	1.199(2.772)	1.938(4.872)	0.179(0.776)
8.0	10	0.633(0.768)	0.750(0.918)	0.152(0.199)
	100	1.000(5.540)	1.585(9.745)	0.098(1.552)
16.0	10	0.903(1.535)	1.041(1.836)	0.187(0.398)
	100	0.920(11.090)	1.019(19.490)	0.052(3.105)

*(); Linear response

Table 5 Normalized value of laminated anisotropic square plates for Case II

q^*	a/h	Nonlinear response		
		w^*	M_{xx}^*	M_{yy}^*
1.0	10	0.194(0.199)	0.055(0.063)	0.066(0.063)
	100	0.754(1.768)	0.125(0.629)	0.547(0.629)
2.0	10	0.359(0.399)	0.088(0.125)	0.132(0.125)
	100	0.620(3.536)	0.129(1.258)	1.550(1.258)
4.0	10	0.575(0.799)	0.093(0.251)	0.243(0.251)
	100	0.572(7.092)	6.096(2.516)	6.230(2.516)
8.0	10	0.695(1.598)	0.096(0.502)	0.451(0.502)
	100	-	-	-
16.0	10	0.612(3.196)	0.920(1.005)	1.134(1.005)
	100	-	-	-

* () ; Linear response, - : Program stopped

Table 6 Normalized value of laminated anisotropic square plates for Case III

q^*	a/h	Nonlinear response		
		w^*	M_{xx}^*	M_{yy}^*
1.0	10	0.097(0.098)	0.129(0.129)	0.006(0.006)
	100	0.616(0.664)	1.216(1.315)	0.036(0.041)
2.0	10	0.194(0.195)	0.256(0.258)	0.011(0.011)
	100	1.050(1.330)	2.059(2.630)	0.059(0.083)
4.0	10	0.384(0.391)	0.507(0.517)	0.022(0.023)
	100	1.420(2.650)	2.762(5.259)	0.079(0.165)
8.0	10	0.682(0.782)	0.899(1.033)	0.036(0.045)
	100	1.360(5.310)	2.659(10.518)	0.103(0.332)
16.0	10	1.064(1.564)	1.384(2.067)	0.048(0.089)
	100	1.120(10.620)	2.082(21.036)	0.204(0.663)

*() ; Linear response

Table 7 Normalized value of laminated anisotropic square plates for Case IV

q^*	a/h	Nonlinear response		
		w^*	M_{xx}^*	M_{yy}^*
1.0	10	0.101(0.101)	0.069(0.070)	0.070(0.070)
	100	0.698(0.826)	0.528(0.705)	0.623(0.705)
2.0	10	0.199(0.203)	0.134(0.140)	0.141(0.139)
	100	1.023(1.652)	0.624(1.410)	0.942(1.410)
4.0	10	0.381(0.405)	0.249(0.279)	0.271(0.279)
	100	1.087(3.304)	0.087(2.821)	1.264(2.820)
8.0	10	0.658(0.810)	0.401(0.559)	0.478(0.559)
	100	0.819(6.609)	-2.156(5.641)	2.950(5.640)
16.0	10	0.914(1.620)	0.436(1.119)	0.715(1.119)
	100	- (13.220)	- (11.282)	-

*() ; Linear response, - ; Program stopped.

plates with non-symmetric stacking sequence.

The normalized stress distributions for Case I-Case IV are shown in Figs. 11-14. In the case of symmetric stacking sequences (Case I and Case III), the stress distribution is symmetric with respect to the mid surface. It is seen that the stress distributions by non-linear analysis have been deviated from those by linear analysis, especially for thin plate cases. This tendency is due to the second-order effect of the vertical displacement on the membrane stress. For the non-symmetric stacking sequences (Case II and Case IV), however, the stress distribution is drastically changed from tensile stress to compressive stress in reference to the mid surface of laminated plates.

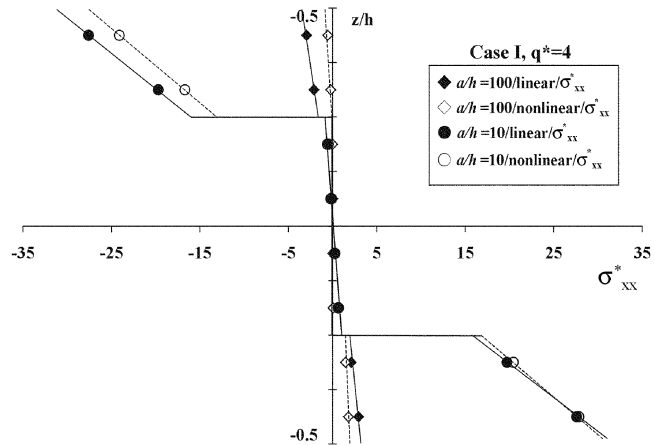


Fig. 11 The non-linear behavior of normalized stress σ_{xx}^* for thin and thick plates in the Case I

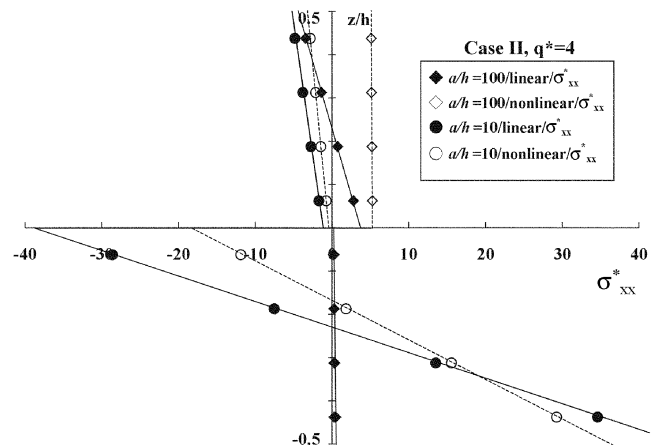


Fig. 12 The non-linear behavior of normalized stresses σ_{xx}^* for thick and thick plates in the Case II

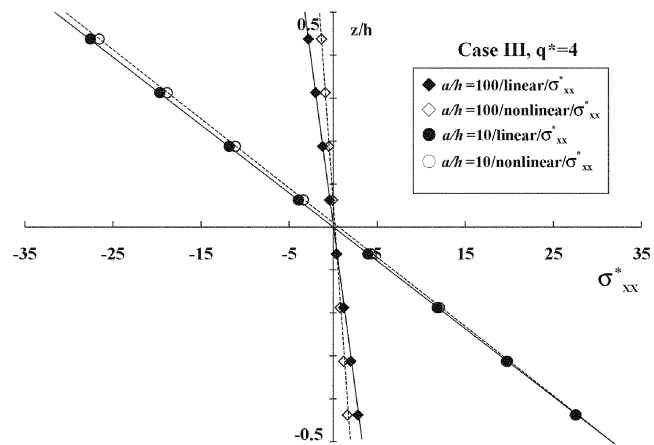


Fig. 13 The non-linear behavior of normalized stress σ_{xx}^* for thin and thick plates in the Case III

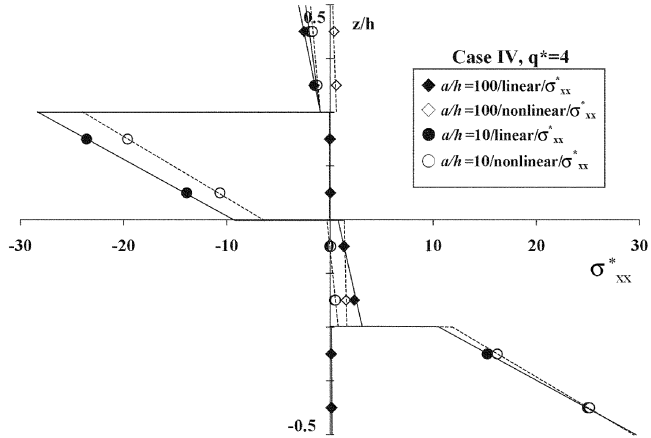


Fig. 14 The non-linear behavior of normalized stress σ_{xx}^* for thick and thick plates in the Case IV

4.2 Laminated anisotropic skew plates

A simply-supported uniformly loaded plate with a skew angle β of 30 degree and equal length sides is analyzed for a range of orientations of the reinforced direction (1-direction). Four p -version finite elements with p -level=5 are used for this problem after the check of convergence tests as shown in Figs. 16-17. To investigate thickness effect, the width/depth ratio, a/h , is selected as 10 for thick case, and 100 for thin case, where h is the thickness of the plate and a is the length of the plate. To keep the same level of central deflection, the applied non-dimensional load q^* is taken as 2 for thin case and 16 for thick case, respectively. The numerical results are based on the same material conditions given in Table 1, and same non-dimensional quantities for bending responses as in previous section.

The maximum non-dimensional deflection and maximum moment at the center of laminated plate are shown in Figs. 18-21 where the fiber orientation α varies from 0° to 180° . The minimum deflection occurs when the direction of reinforcing lies in the direction of the shorter diagonal. On the other hand, the central deflection becomes the maximum when the direction of reinforcing coincides with the longer diagonal. Figs. 20-21 show central moments of the plate with respect to the fiber orientations.

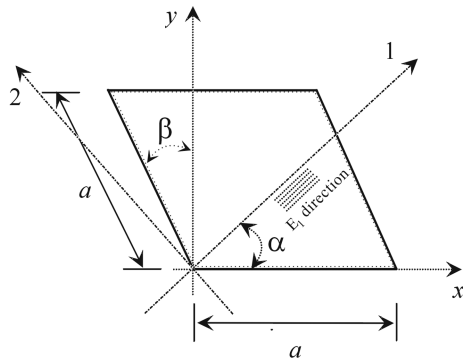


Fig. 15 Simply supported skew plate

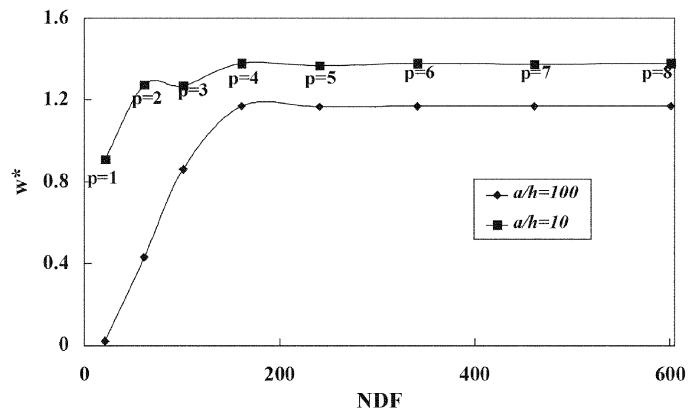


Fig. 16 Convergence characteristics of normalized central deflection of laminated anisotropic skew plates

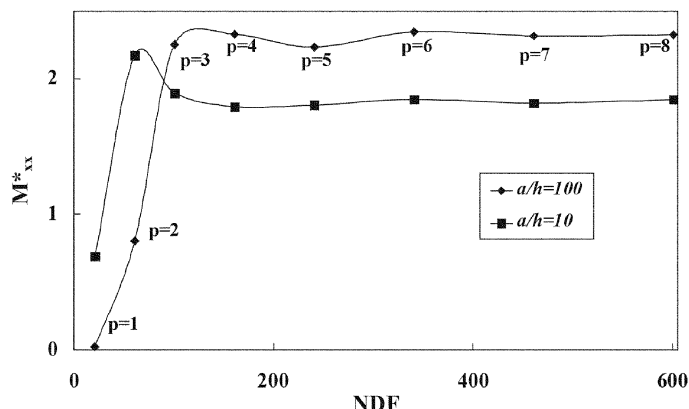
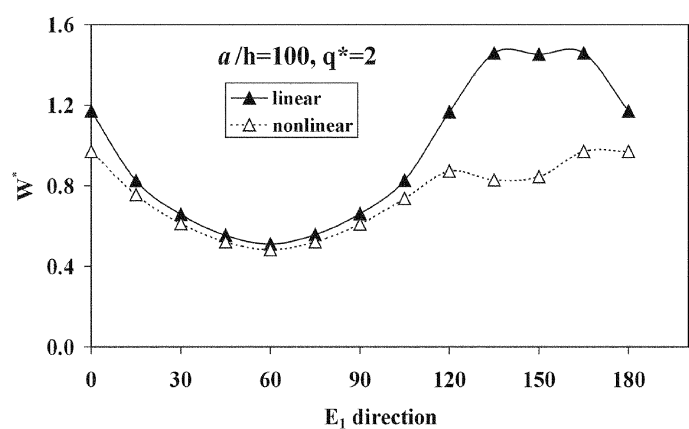


Fig. 17 Convergence characteristics of normalized central moment of laminated anisotropic skew plates

Fig. 18 Variation of central deflection with respect to E_1 direction α when $a/h = 100$ and $q^* = 2$

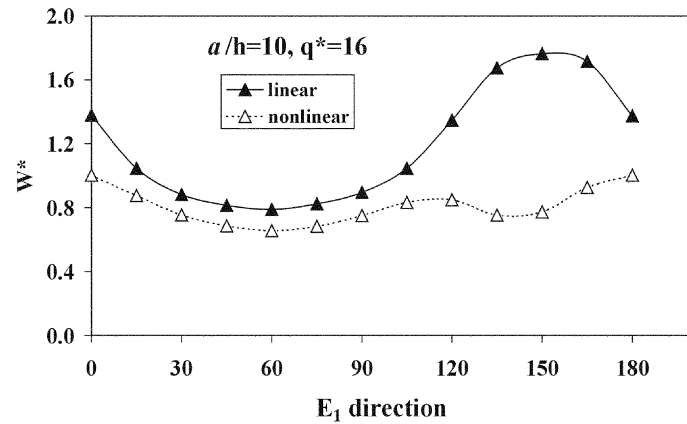


Fig. 19 Variation of central deflection with respect to E_1 direction α when $a/h = 10$ and $q^* = 16$

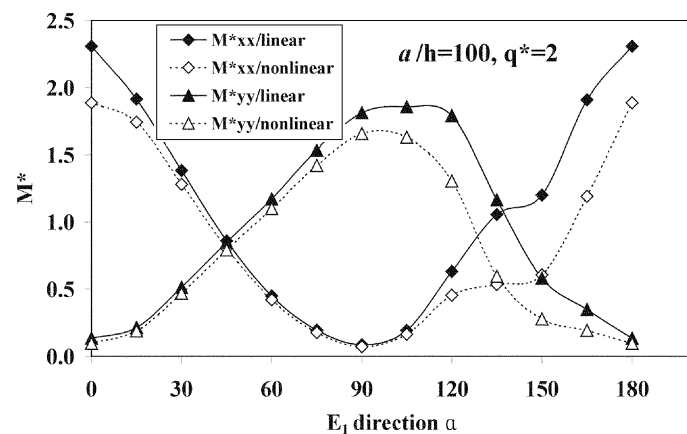


Fig. 20 Variation of central moments with respect to E_1 direction α when $a/h = 100$ and $q^* = 2$

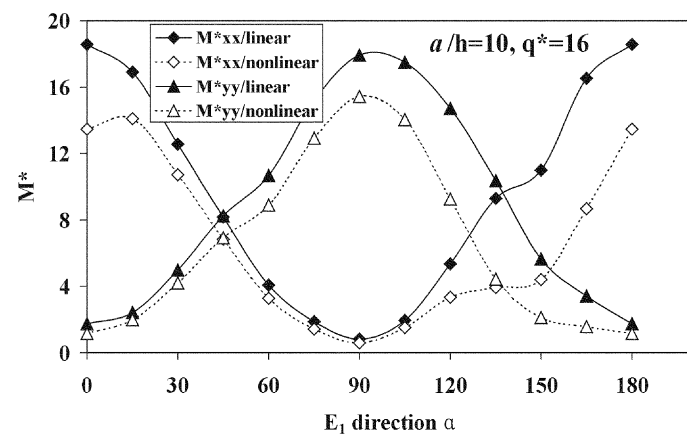


Fig. 21 Variation of central moments with respect to E_1 direction α when $a/h = 10$ and $q^* = 16$

In comparison with the linear analysis, the non-dimensional central deflections by geometric non-linear analysis are reduced for both thin and thick plates. Further, it is noted that the influence of the geometric non-linear effect (or second-order effect) on the lateral deflection is also pronounced when the direction of reinforcing coincides with the longer diagonal.

5. Conclusions

The geometric non-linear static response of anisotropic laminated plates is obtained by the p -version finite element approach. Since the load-deflection curves and load-stress curves indicate that the inclusion of the effect of geometric non-linearity contributes more significantly in the cases of laminated thin plates with non-symmetric stacking sequence and in general, the non-linear analysis is very essential for composite structures. All of the above discussions point out that the p -version finite elements have a good convergence rate and performance for both linear and non-linear deformation. Therefore, the p -version model presented herein offers a reliable tool for the non-linear anisotropic laminated rectangular and skew plates, as demonstrated by parametric studies. However, the theoretical and numerical verifications are needed by other investigators to validate the accuracy of the proposed p -version finite element model.

References

- Actis, R.L., Szabo, B.A. and Schwab, Ch. (1999), "Hierarchic models for laminated plates and shells", *Comput. Meth. Appl. Mech. Engrg.*, **172**, 79-107.
- Fares, M.E. (1999), "Non-linear bending analysis of composite laminated plates using a refined first-order theory", *Composite Structures*, **46**, 257-266.
- Holzer, S. and Yosibash, Z. (1996), "The p -version of finite element methods in incremental elasto-plastic analysis", *Numer. Meth. Engng.*, **39**, 1859-1878.
- Krause, R., Mucke, R. and Rank, E. (1995), " hp -Version finite elements for geometrically nonlinear problems", *Communications in Numer. Meth. Eng.*, **101**, 887-897.
- Liu, J.H. and Surana, K.S. (1995), "A p -version curved shell element based on piecewise hierarchical displacement approximation for laminated composite plates and shells", *Comput. Struct.*, **55**(3), 527-542.
- Liu, R.H., Xu, J.C. and Zhai, S.Z. (1997), "Large-deflection bending of symmetrically laminated orthotropically elliptical plates including transverse shear", *Archiv. Appl. Mech.*, **67**, 507-520.
- Madenci, E. and Barut, A. (1994), "A free-formulation-based flat shell element for non-linear analysis of composite structures", *Numer. Meth. Engng.*, **37**, 3825-3842.
- Owen, D.R.J. and Figueiras, J.A. (1983), "Anisotropic elasto-plastic finite element analysis of thick and thin plates and shells", *Numer. Meth. Engng.*, **19**, 541-566.
- Owen, D.R.J. and Li, Z.H. (1987), "A refined analysis of laminated plates by finite element displacement methods-I. fundamentals and static analysis", *Comput. Struct.*, **26**(6), 907-914.
- Rank, E., Krause, R. and Preusch, K. (1998), "On the accuracy of p -version elements for the Reissner-Mindlin plate problem", *Numer. Meth. Engng.*, **43**, 51-67.
- Reddy, J.N. (1984), "Exact solution of moderately thick laminated shells", *Engineering Mechanics*, ASCE, **110**, 794-809.
- Reddy, J.N. (1997), *Mechanics of Laminated Composite Plates: Theory and Analysis*, CRC Press.
- Schwartz, M. (1992), *Composite Materials Handbook*. 2nd Ed., McGraw-Hill.
- Szabo, B. and Babuska, I. (1991), *Finite Element Analysis*, John Wiley & Sons, Inc.
- Timoshenko, S. and Woinowsky, K.S. (1959), *Theory of Plates and Shells*. 2nd Ed., McGraw-Hill.
- Woo, K.S. (1993), "Robustness of hierarchical elements formulated by integrals of Legendre polynomials", *Comput. Struct.*, **49**, 421-426.